Theoretical study of radiative and non-radiative decay processes in pyrazine derivatives

Chunmei Deng, Yingli Niu, Qian Peng, Anjun Qin, Zhigang Shuai, and Ben Zhong Tang

Citation: The Journal of Chemical Physics **135**, 014304 (2011); doi: 10.1063/1.3606579
View online: https://doi.org/10.1063/1.3606579
View Table of Contents: http://aip.scitation.org/toc/jcp/135/1
Published by the American Institute of Physics

Theoretical study of radiative and non-radiative decay processes in pyrazine derivatives

Chunmei Deng,[1,2] Yingli Niu,[1] Qian Peng,[1,a)] Anjun Qin,[3] Zhigang Shuai,[1,4] and Ben Zhong Tang[2,3,b)]

[1]*Key Laboratory of Organic Solids, Beijing National Laboratory for Molecular Science (BNLMS), Institute of Chemistry, Chinese Academy of Sciences, 100190 Beijing, People's Republic of China*
[2]*Department of Chemistry, The Hong Kong University of Science & Technology, Clear Water Bay, Kowloon, Hong Kong, People's Republic of China*
[3]*MoE Key Laboratory of Macromolecular Synthesis and Functionalization, Department of Polymer Science and Engineering, Zhejiang University, 310027 Hangzhou, People's Republic of China*
[4]*Department of Chemistry, Tsinghua University, 100084 Beijing, People's Republic of China*

(Received 26 March 2011; accepted 13 June 2011; published online 7 July 2011)

Aggregation-induced emission (AIE) phenomenon has attracted much attention in recent years due to its potential applications in optoelectronic devices, fluorescence sensors, and biological probes. Restriction of intramolecular rotation has been proposed as the cause of this unusual phenomenon. Rational design of AIE luminogens requires quantitative descriptions of its mechanism. 2,3-dicyano-5,6-diphenylpyrazine (DCDPP) with "free" phenyl rings is an AIE active compound, whereas 2,3-dicyanopyrazino [5,6-9,10] phenanthrene (DCPP) with "locked" phenyl rings is not. Quantum chemistry calculations coupled with our thermal vibration correlation function formalism for the radiative and non-radiative decay rates reveal that the radiative decay rates for both DCPP and DCDPP are close to each other for all the temperatures, but the non-radiative decay processes are very different. For DCDPP, the low-frequency modes originated from the phenyl ring twisting motions are strongly coupled with the electronic excited state, which dissipate the electronic excitation energy through mode-mixing (Duschinsky rotation effect), and the non-radiative decay rate strongly increases with temperature. For DCPP, however, such mode-mixing effect is weak and the non-radiative decay rate is insensitive to temperature. These findings rationalize the fact that DCDPP is AIE active but DCPP is not, and are instructive to further development of AIE luminogens. © *2011 American Institute of Physics*. [doi:10.1063/1.3606579]

I. INTRODUCTION

Since the aggregation-induced emission (AIE) phenomenon was reported by Tang *et al.* in 2001, it has attracted increasing attentions.[1,2] A variety of organic molecules have been shown to demonstrate the AIE effect, which include siloles,[2–6] tetraphenylethene,[2,7–9] fluorene derivatives,[10,11] etc. Optoelectronic devices, such as organic light-emitting diodes[12–15] and photovoltaic cells,[16] operate in solid state. Molecules with AIE property are thus promising to achieve superior performances in the optoelectronic devices. Furthermore, AIE molecules with functional groups can be utilized as chemosensors and bioprobes with high sensitivity and selectivity, for example, in the fluorescent detection of D-glucose[17] and the quantization of carbon dioxide.[18] To advance the AIE research, it is of utmost interest to gain microscopic insights into the AIE processes.

Several mechanisms have been proposed to explain the AIE processes, including the restriction of intramolecular rotation,[19,20] formation of J-aggregates,[21,22] excimer formation,[23] intramolecular planarization,[24] and twisting intramolecular charge transfer.[25] In order to better understand the AIE phenomena, it is necessary to carry out theoretical and computational studies to quantitatively describe the electronic processes in these systems.

The AIE phenomenon was first investigated theoretically through the first-principles calculations with the excited state vibronic coupling for silole derivatives.[26,27] It was found that the couplings arising from the low-frequency motions contribute the most to the non-radiative decay process and it was conjectured that these motions are easily hindered by solid state packing. More quantitatively, it has been shown that these low-frequency modes are strongly coupled to each other through Duschinsky rotation effects (DRE) at the lowest excited electronic state parabola, which dissipates the excitation energy very efficiently for the molecules with AIE characteristics,[28,29] as evidenced by the comparative studies of 1,2,3,4-tetraphenyl-1,3-butadiene, 1,1,4,4-tetraphenyl-butadiene[28] and 9-[(*o*-aminophenyl)phenylmethylene]-9H-fluorene.[29] These investigations have been based on our recently developed vibration correlation function formula[30,31] for the internal conversion rate process coupled with the first-principles quantum chemistry calculations. Such an approach has been shown to give quantitative descriptions both for the radiative and the non-radiative decay processes.[29,32]

Recently, Qin *et al.* synthesized a pair of pyrazine derivatives named 2,3-dicyano-5,6-diphenylpyrazine (DCDPP)

a)Electronic mail: qpeng@iccas.ac.cn.
b)Electronic mail: tangbenz@ust.hk.

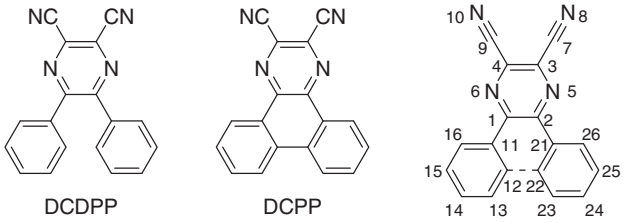

FIG. 1. Chemical structures of DCDPP and DCPP, the atom-labeling scheme is shown at the right.

and 2,3-dicyanopyrazino [5,6-9,10] phenanthrene (DCPP; Fig. 1).[33] It was found that the fluorescence quantum yield of DCDPP is 0.015% in pure tetrahydrofuran (THF) solution, while it is increased 25 times when water is added to THF up to 90% in content: due to the big difference in polarity, the solute molecules start to aggregate. That is to say, DCDPP showed a pronounced AIE effect. Whereas, DCPP in THF solution is intensely emissive, and the addition of water into the THF solution only leads to a normal PL quenching, indicating that DCPP is a non-AIE compound. As can been seen from Fig. 1, the difference in molecular structure is that the two phenyl rings in DCDPP are linked through a single bond in DCPP. We here present a computational study on the photophysical properties of these two molecules, to reveal the microscopic origin of the AIE phenomenon in a quantitative way.

II. METHODOLOGY AND COMPUTATIONAL SCHEMES

According to the Jablonski diagram, there are three major de-excitation pathways for the first singlet excited state (S_1): (i) the radiative decay from S_1 to the ground state (S_0) with a rate k_r, (ii) the non-radiative internal conversion (IC) process from S_1 to S_0 with a rate k_{IC}, and (iii) the intersystem crossing (ISC) process from S_1 to the first triplet excited states (T_1) with a rate k_{ISC}. Thus, the fluorescence quantum yields (Φ_F) are defined as the competition between radiative decay and non-radiative decay from the first singlet excited state to the ground state:[34]

$$\Phi_F = \frac{k_r}{k_r + k_{nr}} = \frac{k_r}{k_r + k_{IC} + k_{ISC}}. \tag{1}$$

The radiative decay rate k_r can be obtained by the integration over the wavelength of the emission spectrum:

$$k_r(T) = \int \sigma_{emi}(\omega, T)\mathrm{d}\omega, \tag{2}$$

where

$$\sigma_{emi}(\omega, T) = \frac{4\omega^3}{3\hbar c^3} \sum_{v_i, v_f} P_{iv_i}(T) |\langle \Theta_{f,v_f} | \mu_{fi} | \Theta_{i,v_i} \rangle|^2 \delta(\omega_{iv_i fv_f} - \omega). \tag{3}$$

$\mu_{fi} = \langle \Phi_f | \vec{\mu} | \Phi_i \rangle$ is the electric transition dipole moment, and can be expanded in a Taylor series in the normal coordinates, $\mu_{fi} = \mu_0 + \sum_k \mu_k Q_k + \sum_{kl} \mu_{kl} Q_k Q_l + O(Q^3)$. Considering the strongly allowed transitions of the molecules in this paper, only the zeroth-order term is taken into account, even though our formalism has included the Herzberg-Teller term;[32] P_{iv_i} is the Boltzmann distribution function for the initial state vibronic manifold; Φ and Θ are the electronic and vibrational wavefunctions, respectively.

Under the Franck-Condon approximation, using Fourier transformation of delta function, Eq. (3) becomes

$$\sigma_{em}^{FC}(\omega) = \frac{2\omega^3}{3\pi\hbar c^3} |\mu_0|^2 \int_{-\infty}^{\infty} e^{-i(\omega - \omega_{if})t} Z_{iv}^{-1} \rho_{em,0}^{FC}(t, T)\mathrm{d}t. \tag{4}$$

Here,

$$\rho_{em,0}^{FC}(t, T) = \mathrm{Tr}[e^{-i\tau_f \hat{H}_f} e^{-i\tau_i \hat{H}_i}] \tag{5}$$

is the thermal vibration correlation function, with $\tau_f = t/\hbar$, $\tau_i = -i\beta - \tau_f$, and $\beta = (k_B T)^{-1}$, and $H_{f(i)}$ is the final (initial) state Hamiltonian of multi-dimensional harmonic oscillators, with which Eq. (4) can be solved analytically by virtue of Gaussian integration through the correlation function as

$$\rho_{em,0}^{FC}(t, T) = \sqrt{\frac{\det[\mathbf{a}_f \mathbf{a}_i]}{\det[\mathbf{K}]}} \exp\left\{ -\frac{i}{\hbar} \left[\frac{1}{2} \underline{F}^T \mathbf{K} \underline{F} - \underline{D}^T \mathbf{E} \underline{D} \right] \right\}, \tag{6}$$

where $\mathbf{a}_i$, $\mathbf{a}_f$, and $\mathbf{E}$ are $N \times N$ matrices, $\mathbf{K}$ is $2N \times 2N$ matrix, $\underline{D}$ and $\underline{F}$ are $N \times 1$ and $2N \times 1$ matrices, respectively, with all of the mathematical forms given in Ref. 32. This formalism was recently applied to the molecular design of efficient infrared emissive materials.[35]

The internal conversion rate can be evaluated through the Fermi-Golden Rule expressed as

$$k_{IC} = \frac{2\pi}{\hbar} |H'_{fi}|^2 \delta(E_f - E_i), \tag{7}$$

$$H'_{fi} = -\hbar^2 \sum_l \left\langle \Phi_f \Theta_{fv_f} \left| \frac{\partial \Phi_i}{\partial Q_{fl}} \frac{\partial \Theta_{iv_i}}{\partial Q_{fl}} \right\rangle \right., \tag{8}$$

where H'denotes the Born-Oppenheimer coupling due to the breakdown of the adiabatic approximation.[36] Φ denotes the electronic wavefunction, and Θ represents the nuclear vibration wavefunction. l is the normal mode index and i(f) denotes the initial (final) state. Thus, operator H'serves as a transition coupling between two electronic states due to the nuclear vibrational perturbation.

The relationship between the normal coordinates of the two coupled electronic state parabolas is expressed by a linear transformation:

$$Q_i = \mathbf{S} Q_f + \underline{D}. \tag{9}$$

Here, $\underline{D}$ is the (3*N*–6)-dimensional normal coordinate displacement vector, and $\mathbf{S}$ is the (3*N*–6) × (3*N*–6)-dimensional Duschinsky rotation matrix, or potential energy surface distortion matrix. The elements of $\mathbf{S}$ represent the mixing of normal modes in the initial and final electronic states. This matrix characterizes the vibrational mode mixings upon electronic excitation. Under the rigid displacement approximation, $\mathbf{S}$ becomes a delta-function, which has been widely assumed for understanding the optical spectrum of polyatomic molecules, namely, the parabola of the ground state and the excited state are different only at the origins in the normal mode coordinate space. As we pointed out previously, for molecules

TABLE I. Selected bond lengths (L, in Å), bond angles (A, in degree), and dihedral angles (D, in degree) for DCDPP and DCPP in their ground states (S_0) and the first singlet excited states (S_1). S_1–S_0 represents the difference between S_1 and S_0.

	DCDPP			DCPP		
	S_0	S_1	S_1–S_0	S_0	S_1	S_1–S_0
L(C1−C2)	1.439	1.471	0.032	1.428	1.386	−0.042
L(C3−C4)	1.416	1.471	0.056	1.425	1.412	−0.013
L(C1−N6)	1.335	1.337	0.002	1.340	1.367	0.027
L(C4−N6)	1.332	1.323	−0.008	1.326	1.353	0.026
L(C4−C9)	1.442	1.430	−0.012	1.443	1.440	−0.003
L(C1−C11)	1.486	1.453	−0.033	1.457	1.465	0.007
L(C12−C22)				1.472	1.428	−0.044
A(C2−C1−C11)	125.2	123.0	−2.2	120.3	119.6	−0.7
D(C2−C1−C11−C12)	36.0	20.0	−16.0	0.0	0.0	0.0

with floppy motions coupled with the electronic excitations, the Duschinsky rotation effect can largely influence the non-radiative decay processes upon increasing the phonon occupation (temperature).[28,29] Recent combined computational and experimental investigations showed that in order to achieve quantitative assignments for single vibronic level fluorescence spectroscopy in phenylvinylacetylene, Duschinsky rotation effects are imperial, which posed computational challenges for quantum chemistry.[37,38]

Under the Franck-Condon approximation, the IC rate can be expressed as

$$k_{\mathrm{IC}} = \sum_{kl} k_{\mathrm{IC},kl} = \sum_{kl} \frac{2\pi}{\hbar} R_{kl} Z_{\mathrm{iv}}^{-1} \sum_{v_{\mathrm{i}},v_{\mathrm{f}}} e^{-\beta E^{\mathrm{i}}_{v_{\mathrm{i}}}} P_{kl} \delta\left(E_{\mathrm{if}} + E^{\mathrm{i}}_{v_{\mathrm{i}}} - E^{\mathrm{f}}_{v_{\mathrm{f}}}\right). \tag{10}$$

Here,

$$R_{kl} = \langle \Phi_{\mathrm{f}} | \hat{P}_{\mathrm{f}k} | \Phi_{\mathrm{i}} \rangle \langle \Phi_{\mathrm{i}} | \hat{P}_{\mathrm{f}l} | \Phi_{\mathrm{f}} \rangle \tag{11}$$

is the non-adiabatic electronic coupling due to nuclear momentum P, and

$$P_{kl} = \langle \Theta_{\mathrm{f}} | \hat{P}_{\mathrm{f}k} | \Theta_{\mathrm{i}} \rangle \langle \Theta_{\mathrm{i}} | \hat{P}_{\mathrm{f}l} | \Theta_{\mathrm{f}} \rangle. \tag{12}$$

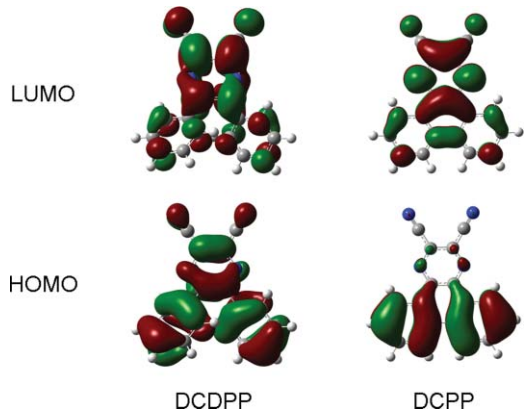

FIG. 2. Spatial distributions of the LUMO and HOMO for DCDPP and DCPP.

TABLE II. Effect of temperature on radiative (k_{r}) and internal conversion rates (k_{IC}) and fluorescence quantum yield (Φ_{F}) of DCDPP, "no DRE" means without considering DRE.

	k_{r} (10^7 s^{-1})		k_{IC} (s^{-1})		Φ_{F} (%)	
T (K)	DRE	no DRE	DRE (10^8)	no DRE	DRE	no DRE
300	0.932	1.33	44.5	695	0.21	99.99
250	0.983	1.33	24.4	391	0.40	100.00
200	1.04	1.33	12.1	655	0.85	100.00
150	1.09	1.33	5.32	763	2.00	99.99
100	1.14	1.33	2.14	471	5.05	100.00
77	1.16	1.33	1.40	457	7.62	100.00
50	1.18	1.33	9.01	739	11.60	99.99
20	1.20	1.33	6.75	567	15.09	100.00

Applying the Fourier transformation, the IC becomes

$$k_{\mathrm{IC}} = \sum_{kl} \frac{1}{\hbar^2} R_{kl} \int_{-\infty}^{\infty} \mathrm{d}t [e^{i\omega_{\mathrm{if}}t} Z_{\mathrm{iv}}^{-1} \rho_{\mathrm{IC},kl}(t,T)], \tag{13}$$

where,

$$\rho_{\mathrm{IC},kl}(t,T) = \mathrm{Tr}[\hat{P}_{\mathrm{f}k} e^{-i\tau_{\mathrm{f}}\hat{H}_{\mathrm{f}}} \hat{P}_{\mathrm{f}l} e^{-i\tau_{\mathrm{i}}\hat{H}_{\mathrm{i}}}] \tag{14}$$

is the IC thermal vibration correlation function. The derived analytical expression is given as

$$\rho_{\mathrm{IC},kl}(t,T) = \sqrt{\frac{\det[\mathbf{a}_{\mathrm{f}}\mathbf{a}_{\mathrm{i}}]}{\det[\mathbf{K}]}} \exp\left\{-\frac{i}{\hbar}\left[\frac{1}{2}\underline{F}^{\mathrm{T}}\mathbf{K}^{-1}\underline{F} - \underline{D}^{\mathrm{T}}\mathbf{E}\underline{D}\right]\right\} \times\left\{i\hbar\mathrm{Tr}\left[\mathbf{G}^{\mathrm{IC}}_{kl}\mathbf{K}^{-1}\right] + (\mathbf{K}^{-1}\underline{F})^{\mathrm{T}} \times\mathbf{G}^{\mathrm{IC}}_{kl}(\mathbf{K}^{-1}\underline{F}) - \left(\underline{H}^{\mathrm{IC}}_{kl}\right)^{\mathrm{T}}\mathbf{K}\right\}, \tag{15}$$

where, $\mathbf{G}^{\mathrm{IC}}_{kl}$ and $\underline{H}^{\mathrm{IC}}_{kl}$ are the $(2N \times 2N)$ and $(1 \times 2N)$ matrices, respectively. The details of the correlation function are derived in Refs. 31 and 32.

For the electronic coupling part of IC rate,[30,32] we apply the first-order perturbation theory following Lin,[39]

$$\langle \Phi_{\mathrm{f}} | \frac{\partial}{\partial Q_{\mathrm{fl}}} | \Phi_{\mathrm{i}} \rangle = \frac{\langle \Phi^0_{\mathrm{f}} | \partial V / \partial Q_{\mathrm{fl}} | \Phi^0_{\mathrm{i}} \rangle}{E^0_{\mathrm{i}} - E^0_{\mathrm{f}}}, \tag{16}$$

where

$$\langle \Phi^0_{\mathrm{f}} | \partial V / \partial Q_{\mathrm{fl}} | \Phi^0_{\mathrm{i}} \rangle = -\sum_{\sigma} \frac{Z_\sigma \mathrm{e}^2}{\sqrt{M_\sigma}} \sum_{\tau=x,y,z} E_{\mathrm{j}\leftarrow\mathrm{i},\sigma\tau} L_{\sigma\tau,k}, \tag{17}$$

and the transition field $E_{\mathrm{j}\leftarrow\mathrm{i},\sigma\tau} = \int \mathrm{d}\mathbf{r}\rho_{\mathrm{ji}}(\mathbf{r})(\mathrm{e}(r_\tau - R_{\sigma\tau})/|\mathbf{r} - \mathbf{R}_\sigma|^3)$ can be calculated by complete active space self-consistent field or time-dependent density functional theory (TDDFT).

It should be noted that such formalism can be only applied at potential energy surfaces well away from the conical intersection points. Namely, the ground state and the excited state should not be too close to each other such that the denominator of Eq. (16) does not vanish. In fact, when conical intersection becomes important, the non-adiabatic transition is usually very fast, with a decay rate greater than 10^{12}–10^{13} s^{-1}. Then, quantum dynamics theory should be applied.[40,41] Also, at this stage, we did not consider the ISC process since for many conjugated systems, this is a rather

TABLE III. Effect of temperature on radiative (k_r) and internal conversion rates (k_{IC}) and fluorescence quantum yield (Φ_F) of DCPP, "no DRE" means without considering DRE.

	k_r (10^6 s^{-1})		k_{IC} (10^5 s^{-1})		Φ_F (%)	
T (K)	DRE	no DRE	DRE	no DRE	DRE	no DRE
300	1.59	1.61	3.29	1.70	82.83	90.49
250	1.60	1.62	2.74	1.48	85.36	91.63
200	1.61	1.63	2.42	1.36	86.93	92.27
150	1.61	1.63	2.25	1.30	87.78	92.60
100	1.62	1.64	2.15	1.28	88.27	92.76
77	1.62	1.64	2.13	1.28	88.40	92.76
50	1.62	1.64	2.11	1.27	88.51	92.81
20	1.62	1.64	2.09	1.27	88.60	92.83

slow process compared with the radiative decay process. The typical ISC rate is less than 10^5 s^{-1}, while the radiative decay rate is around 10^7–10^8 s^{-1}.

The S_0 geometry optimization was started with the x-ray crystal structure[33] by using the density functional theory (DFT) and then the TDDFT method was applied to optimize the S_1 geometry. Becke's three-parameter hybrid exchange function with Lee-Yang-Parr gradient corrected correlation functional (B3LYP functional) (Refs. 42 and 43) and the def2-SV(P) (Refs. 44 and 45) basis set were employed throughout the work. Both the energy convergence thresholds for the ground-state and the excited-state optimization were set to be 10^{-8} atomic unit. It should be noted that at this stage, TDDFT with common exchange-correlation functional works well only for the low-lying excited state with mostly single excitation character.[46,47] As is shown in Sec. III, for the molecules we considered here, the lowest excited state consists of primarily highest occupied molecular orbital (HOMO)-lowest unoccupied molecular orbital (LUMO) promotion. Thus, it is appropriate to apply TDDFT. The molecular symmetries are C_2 and C_{2v} for DCDPP and DCPP, respectively. Quantum chemistry calculations were carried out by using the TURBOMOLE 6.0 program.[48–50] The transition electric field of the electronic coupling factor for the internal conversion rate is calculated at the TDDFT level by using GAUSSIAN 03 program package.[51] Based on the electronic structure information, the Duschinsky rotation matrix and the normal mode displacements (D_i) between the two electronic state parabola, as well as the radiative and non-radiative decay rates were calculated.

III. RESULTS AND DISCUSSION

Table I shows the selected bond lengths, bond angles, and dihedral angles of DCDPP and DCPP in both S_0 and S_1 states. The molecular geometry labeling scheme is shown in Fig. 1. From Table I, it is the bond lengths (C3–C4 and C1–C2) which experience remarkable changes for both DCDPP and DCPP when exciting from S_0 to S_1. DCPP maintains almost fully coplanar structure in both S_0 and S_1 states, while in DCDPP the phenyl rings are twisted sharply from 36.0° in S_0 to 20.0° in S_1.

According to our TDDFT results, the S_1 state is dominated by the transition from the HOMO to the LUMO, 96.4% for DCDPP and 94.7% for DCPP. The wavefunctions of the HOMO and LUMO orbitals are shown in Fig. 2. It can be seen that the HOMO for DCDPP is delocalized on the two "free" phenyl rings and the pyrazine ring, while that for DCPP is localized mostly on the two "locked" phenyl rings. The LUMO is mainly originated from the pyrazine ring for both DCDPP and DCPP. Hence, it is expected that the pyrazine ring and the two phenyl rings will affect the photophysical properties of both DCDPP and DCPP. In addition, in the two compounds, the HOMO and LUMO both display the π and π^* characters. Generally, the spin-orbital coupling is very small for the $\pi \rightarrow \pi^*$ electron transition, which rationalized our neglect of the ISC process here.

A. Photophysical properties

Based on DFT and TDDFT calculations for the transition dipole moment and the vibronic coupling, the radiative decay and IC rates and the corresponding fluorescent quantum yields of DCDPP and DCPP are calculated and compared for cases with DRE and without DRE for temperature ranging

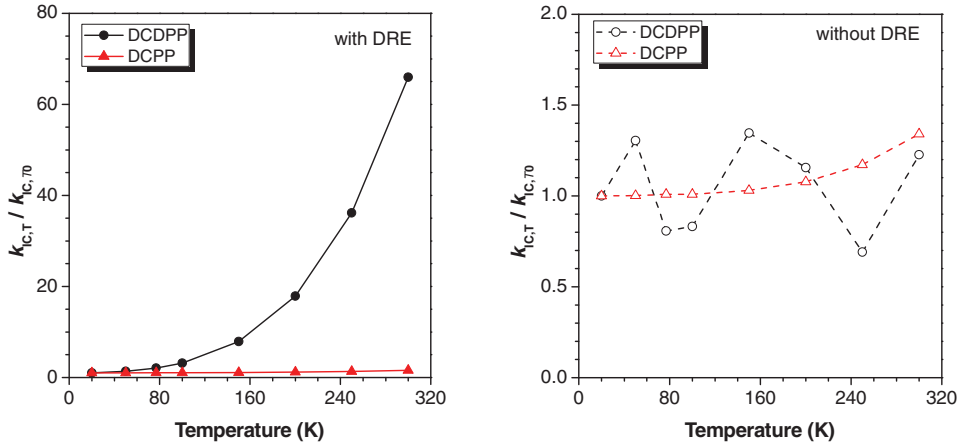

FIG. 3. Temperature dependence of the internal conversion rates normalized at $T0$ ($k_{IC,T}/k_{IC,T0}$), from S_1 to S_0 states of DCDPP and DCPP with DRE (left) and without DRE (right), $T0 = 20$ K.

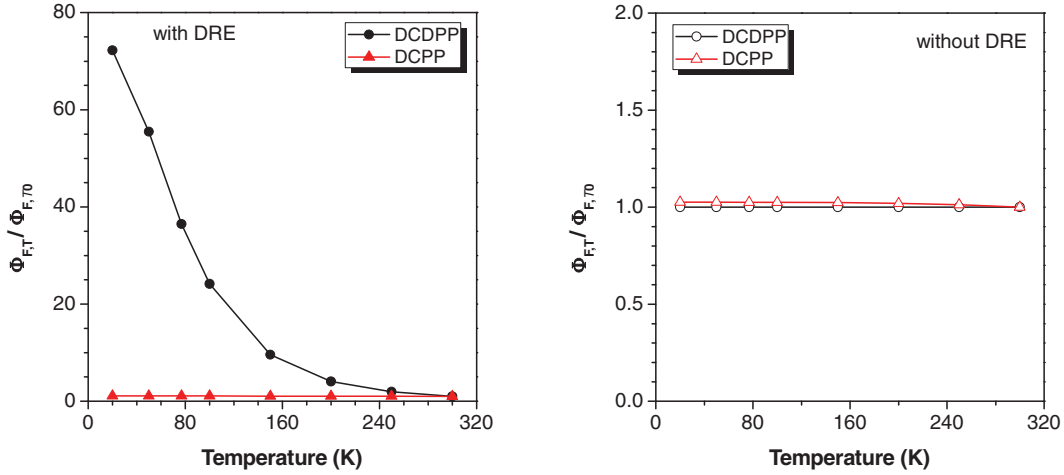

FIG. 4. Temperature dependence of the normalized fluorescence quantum yields ($\Phi_{F,T}/\Phi_{F,T0}$) from S_1 to S_0 states of DCDPP and DCPP, with DRE (left) and without DRE (right), referenced at $T0 = 300$ K.

from 20 K to 300 K. The calculated results are summarized in Tables II and III.

From Tables II and III, it can be seen that at 300 K, the radiative decay rate of DCDPP (9.32×10^6 s^{-1}) is even larger than that of DCPP (1.59×10^6 s^{-1}). Moreover, from 300 K to 20 K, the radiative rate of DCDPP is always larger than that of DCPP. These data suggest that the increase in the emission efficiency from DCDPP to DCPP in THF solution does not stem from the radiative decay process.

In contrast to the radiative process, the IC rate of DCDPP (Table II) is much larger than that of DCPP (Table III) at 300 K (4.45×10^9 s^{-1} vs. 3.29×10^5 s^{-1}) with DRE and the corresponding fluorescence quantum yields are 0.21% and 82.83%, respectively. Thus, it is the dramatic decrease in the IC rate that has brought about the increase in the fluorescent efficiency when going from DCDPP to DCPP. At the same time, it suggests that the luminescent properties can be tuned dramatically by simply changing the molecular structure.

In order to further analyze the temperature dependence, we depict the IC rate normalized to the value at $T0 = 20$ K ($k_{IC,T0}$) in Fig. 3. It is obviously noted that for DCDPP, the inclusion of DRE makes the IC rate enhanced by about 70 times from 20 K to 300 K. If DRE is neglected, the IC rate is found to be insensitive to the temperature. For DCPP, the IC rate hardly varies from 20 K to 300 K, for both with and without considering DRE. The temperature dependence of Φ_F with and without DRE is showed in Fig. 4. For DCDPP, the fluorescence quantum yields are increased about 72 times when the temperature is decreased from 300 K to 20 K with DRE. For DCPP, the fluorescence quantum yields are calculated to be insensitive to the temperature in both cases: with and without considering DRE. These findings are in good agreement with the experimental observations that DCDPP is an AIE molecule but DCPP is not. According to our previous theoretical results,[28] an AIE molecule (e.g., 1,2,3,4-tetraphenyl-1,3-butadiene) shows strong mode-mixing (DRE) and prominent temperature dependence for the IC rate, namely, about 650 times increase from 70 K to 300 K, while for a non-AIE molecule (e.g., 1,1,4,4-tetrephenylbutadiene), the IC rate increases only 7 times. In fact, the IC rate is proportional to the weighted Franck-Condon overlap factor between the initial and final electronic states. If there are only displacements in the origin of the normal mode coordinates, the

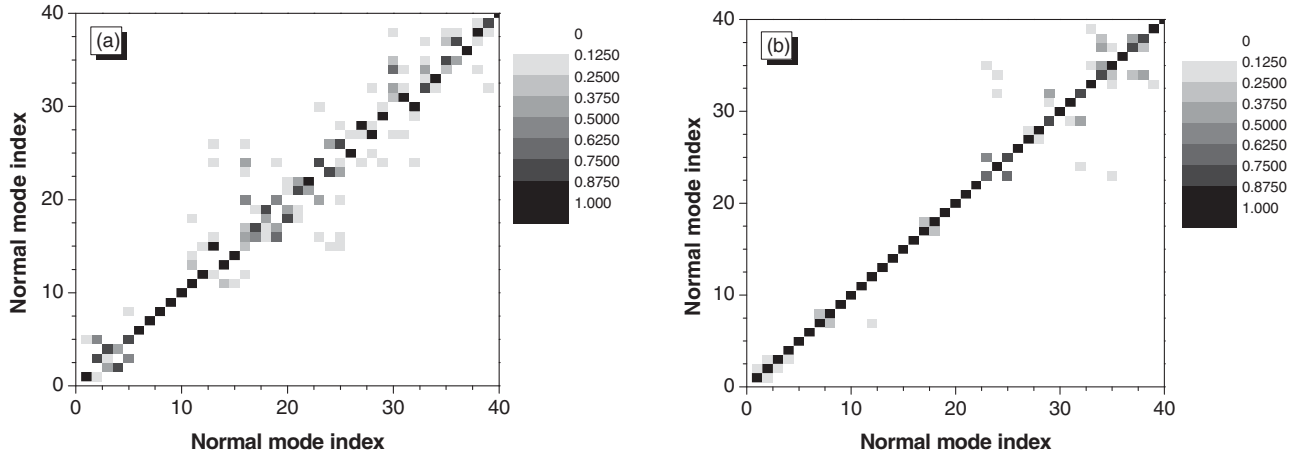

FIG. 5. Contour map of Duschinsky rotation matrix for the lowest 40 normal modes in (a) DCDPP and (b) DCPP.

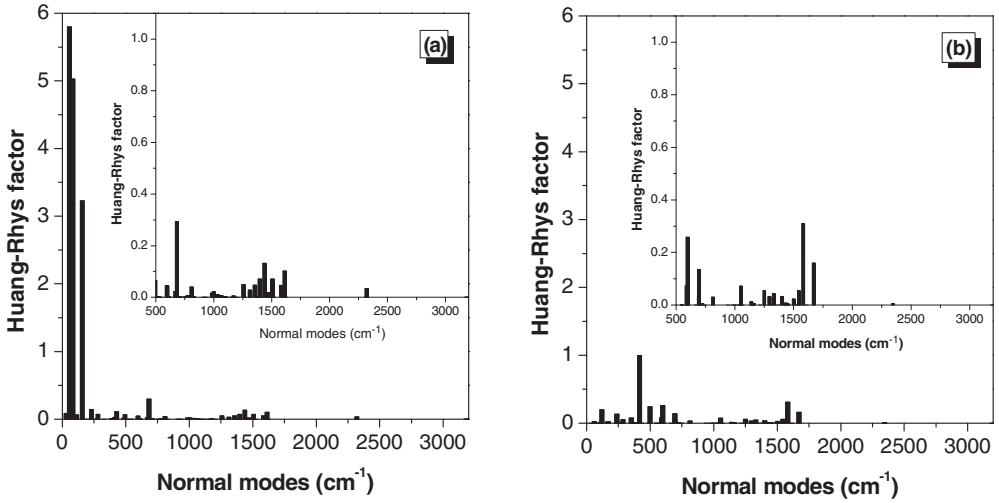

FIG. 6. Huang-Rhys factors for (a) DCDPP and (b) DCPP versus the normal mode wave numbers.

overlap starts to occur amongst vibrational states. Since the modes are independent harmonic oscillators, the overlap can only occur between different quantum states of the same mode. Since temperature can populate the states with larger quanta of vibration, the overlap increases. Once there is a rotation, then in addition to overlaps within the same mode, the overlaps start to spread out to different modes. When temperature is increased, the spread-out effect becomes more and more pronounced due to the vibrational states redistribution to higher quanta and more different modes. This actually explains the more pronounced temperature dependence due to DRE. This is certainly in consistence with the AIE phenomenon. That is, the aggregation tends to hinder the low-frequency twisting motion and to decouple the mode-mixing, thus quenching the IC processes.

The selected contour maps for the absolute values of the Duschinsky rotation matrices for the first forty normal modes ordered with an ascending vibration frequency are presented in Fig. 5 for DCDPP and DCPP, and those for all the normal modes are given in Fig. SI in the supplementary information.[52] By definition, the absolute values of the off-diagonal elements measure the degree of mode-mixing between the two potential energy surface parabola. As shown in Fig. 5, for DCDPP, the Duschinsky rotation matrix elements contain remarkable non-diagonal contributions, while for DCPP, the Duschinsky rotation matrix elements are mainly along the diagonal line. Furthermore, we could also note that, for DCDPP, the mixing of the first five low frequency modes is very large. From the previous studies,[27–29] the contributions from the low frequency motions can cause significant temperature dependence for the IC decay process. Thus, in DCDPP, the IC process and its temperature dependence can be reasonably described when the DRE is considered.

B. Huang-Rhys (HR) factor and reorganization energy

From the previous analysis[27–29] and the schematic descriptions of potential energy surfaces of two electronic states shown in Ref. 53, we know that the HR factor and the reorganization energy are important for non-radiative decay processes. The HR factor $S_i = \omega_i \times D_i^2/2\hbar$ characterizes the averaged number of phonons for the ith normal mode emitted (absorbed) by electron into (from) vibration in the relaxation process. Its reorganization energy (λ_i) is the product of S_i and the corresponding vibration energy: $\lambda_i = S_i \times \hbar\omega_i$.

The HR factors for the lowest singlet excited state of DCDPP and DCPP are presented in panels a and b of Fig. 6, respectively. It is seen that the modes with large HR factors all appear at the low frequency region for DCDPP, e.g., modes 2 (55.76 cm^{-1}), 5 (82.97 cm^{-1}), and 8 (157.25 cm^{-1}), while those for DCPP appear at both low (mode 17, 415.95 cm^{-1}) and high (mode 72, 1582.06 cm^{-1}) frequency regions. Such features again suggest the importance of DRE for DCDPP, because DRE occurs most notably for the low frequency modes.[38] For the sake of clarity, we depict the normal mode displacement vectors for modes with large HR factor: normal modes 2, 5, and 8 of DCDPP and 17 and 72 of DCPP in Fig. 7. Modes 2, 5, and 8 of DCDPP are assigned to the phenyl ring twisting, and mode 72 of DCPP belongs to the stretching vibrations of carbon-carbon bonds.

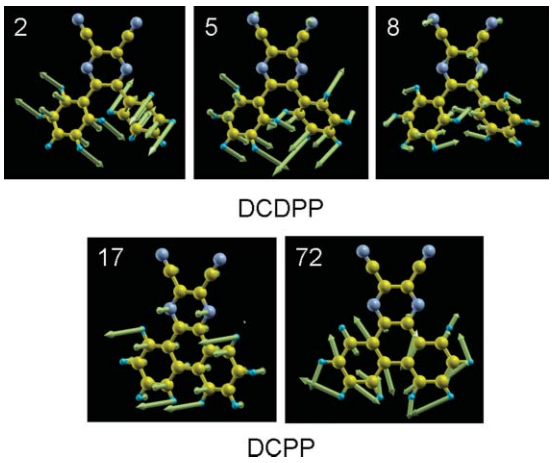

FIG. 7. Diagrammatic illustrations of the normal mode displacement vectors for the selected vibrational normal modes of DCDPP and DCPP.

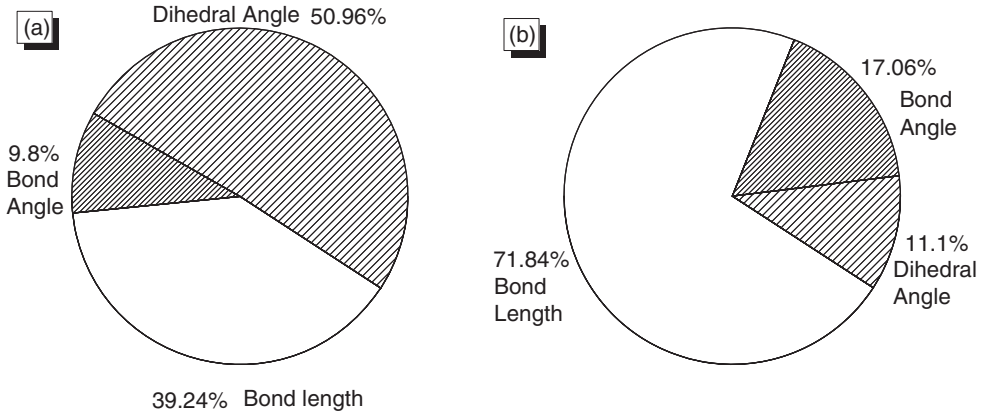

FIG. 8. Contributions to the total reorganization energy from bond length, bond angle, and dihedral angle of (a) DCDPP and (b) DCPP.

Selected reorganization energy (>10 cm^{-1}), the corresponding vibrational frequency, and the displacement for DCDPP and DCPP are shown in Tables SI and SII in the supplementary information.[52] The total reorganization energy is 2677.92 cm^{-1} for DCDPP and 2202.45 cm^{-1} for DCPP. For AIE molecule DCDPP, the low frequency vibrational modes 2, 5, and 8 related to the phenyl ring twisting contribute about 46.6% to the total reorganization energy. According to our previous work, energy dissipation pathways via low-frequency motions are easily quenched in aggregation or at lower temperature, leading to the AIE effect. Hence, the phenyl ring twisting is at the origin of the AIE phenomenon of DCDPP.

To further understand the relationship between the photophysical properties and the molecular structures, we project the reorganization energies onto the internal coordinate of the molecules, and the reorganization energies contributed from bond length, bond angle, and dihedral angle are summarized in Fig. 8. The detailed internal coordinates with large component of reorganization energy (>50 cm^{-1} for DCDPP and >40 cm^{-1} for DCPP) are listed in Table SIII.[52] From Fig. 8, it is noted that the main contributions come from the dihedral angle (50.96%) relating to the rotation motions of the phenyl ring and the bond length (39.24%) for DCDPP, while for DCPP, those are mainly from the bond length (71.84%) associated with the C–C stretching vibrations. These results further confirm that the rotation motion of the phenyl pendants attached to the parent pyrazine core is crucial to determine the luminescent property.

It should be noted that our explanation for the AIE phenomena is so far confined to single molecular excited processes. This is because that in most of the AIE system, the absorption and emission peaks do not shift apparently when going from dilute solution to aggregate. We note that the exciton effect has been widely explored by Spano *et al.* in the context of exciton-phonon coupling at the two-particle approximation, where photophysical properties have been elucidated through influences of the diagonal disorders arising from the phenyl ring rotations on the radiative process for either H or J-aggregates.[54,55] In such circumstance, it is expected that there occurs prominent shifts in either emission or absorption maximum upon aggregation.

IV. CONCLUSIONS

To summarize, we have calculated the radiative and non-radiative decay rates and their temperature dependences for two pyrazine derivatives, DCDPP and DCPP, based on the vibration correlation formula we developed earlier and DFT calculations. At room temperature (300 K), the fluorescence quantum yields of DCDPP and DCPP are calculated to be 0.21% and 82.83%, respectively, indicating that restriction of the phenyl ring rotations in the pyrazine derivatives plays a crucial role in governing their photophysical behaviors, in good agreement with the experimental results.[33] Upon lowering the temperature from 300 K to 20 K, the radiative decay rates for both compounds vary appreciably. However, the Duschinsky rotation from the low-frequency mode mixings enhances the fluorescence quantum yield of DCDPP by 72 times, but exerts little effect on the luminescence efficiency of DCPP. The importance of the phenyl ring twisting motion in DCDPP is found to be essential in understanding its luminescent property, which rationalizes the "restriction of intramolecular rotation" mechanism proposed by Tang *et al.*[19,20] to explain the exotic AIE phenomena. The rotations of the phenyl rings, corresponding to the low frequency vibrational modes, were easily suppressed at the low temperature, which effectively block the non-radiative decay pathways.

ACKNOWLEDGMENTS

This work is supported by the National Natural Science Foundation of China (Grant Nos. 90921007 and 20903102), the Ministry of Science and Technology of China through 973 Program (2009CB623600), and the Research Grants Council of Hong Kong (HKUST2/CRF/10).

[1] J. D. Luo, Z. L. Xie, J. W. Y. Lam, L. Cheng, H. Y. Chen, C. F. Qiu, H. S. Kwok, X. W. Zhan, Y. Q. Liu, D. B. Zhu, and B. Z. Tang, Chem. Commun. (Cambridge), **2001** 1740.
[2] Y. Hong, J. W. Y. Lam, and B. Z. Tang, Chem. Commun. (Cambridge), **2009** 4332; J. Liu, J. W. Y. Lam, and B. Z. Tang, J. Inorg. Organomet. Polym. **19**, 249 (2009); M. Wang, G. X. Zhang, D. Q. Zhang, D. B. Zhu, and B. Z. Tang, J. Mater. Chem. **20**, 1 (2010); Z. Zhao, J. W. Y. Lam, and B. Z. Tang, Curr. Org. Chem. **14**, 2109 (2010).
[3] Y. Ren, J. W. Y. Lam, Y. Dong, B. Z. Tang, and K. S. Wong, J. Phys. Chem. B **109**, 1135 (2005).

[4]X. Fan, J. Sun, F. Wang, Z. Chu, P. Wang, Y. Dong, R. Hu, B. Z. Tang, and D. Zou, Chem. Commun. (Cambridge) **2008**, 2989.
[5]Z. Li, Y. Q. Dong, J. W. Y. Lam, J. Sun, A. Qin, M. Häußler, Y. P. Dong, H. H. Y. Sung, I. D. Williams, H. S. Kwok, and B. Z. Tang, Adv. Funct. Mater. **19**, 905 (2009).
[6]Z. Zhao, Z. Wang, P. Lu, C. Y. K. Chan, D. Liu, J. W. Y. Lam, H. H. Y. Sung, I. D. Williams, Y. Ma, and B. Z. Tang, Angew. Chem., Int. Ed. **48**, 7608 (2009).
[7]H. Tong, Y. Hong, Y. Q. Dong, M. Häußler, J. W. Y. Lam, Z. Li, Z. Guo, Z. Guo, and B. Z. Tang, Chem. Commun. (Cambridge) **2006**, 3705.
[8]Z. Zhao, S. Chen, J. W. Y. Lam, P. Lu, Y. Zhong, K. S. Wong, H. S. Kwok, and B. Z. Tang, Chem. Commun. (Cambridge) **46**, 2221 (2010).
[9]W. Wang, T. Lin, M. Wang, T. X. Liu, L. Ren, D. Chen, and S. Huang, J. Phys. Chem. B **114**, 5983 (2010).
[10]H. Tong, Y. Q. Dong, M. Häußler, J. W. Y. Lam, H. H. Y. Sung, I. D. Williams, J. Sun, and B. Z. Tang, Chem. Commun. (Cambridge) **2006**, 1133.
[11]H. Tong, Y. Q. Dong, Y. Hong, M. Häußler, J. W. Y. Lam, H. H. Y. Sung, X. Yu, J. Sun, I. D. Williams, H. S. Kwok, and B. Z. Tang, J. Phys. Chem. C **111**, 2287 (2007).
[12]C. W. Tang and S. A. Van Slyke, Appl. Phys. Lett. **51**, 913 (1987).
[13]J. H. Burroughes, D. D. C. Bradley, A. R. Brown, R. N. Marks, K. Mackay, R. H. Friend, P. L. Burn, and A. B. Holmes, Nature (London) **347**, 539 (1990).
[14]R. H. Friend, R. W. Gymer, A. B. Holmes, J. H. Burroughes, R. N. Marks, C. Taliani, D. D. C. Bradley, D. A. Dos Santos, J. L. Bredas, M. Logdlund, and W. R. Salaneck, Nature (London) **397**, 121 (1999).
[15]L. S. Hung and C. H. Chen, Mater. Sci. Eng. R **39**, 143 (2002).
[16]Y.-J. Cheng, S.-H. Yang, and C.-S. Hsu, Chem. Rev. **109**, 5868 (2009).
[17]Y. Liu, C. Deng, L. Tang, A. Qin, R. Hu, J. Z. Sun, and B. Z. Tang, J. Am. Chem. Soc. **133**, 660 (2011).
[18]Y. Liu, Y. Tang, N. N. Barashkov, I. S. Irgibaeva, J. W. Y. Lam, R. Hu, D. Birimzhanova, Y. Yu, and B. Z. Tang, J. Am. Chem. Soc. **132**, 13951 (2010).
[19]J. Chen, C. C. W. Law, J. W. Y. Lam, Y. P. Dong, S. M. F. Lo, I. D. Williams, D. Zhu, and B. Z. Tang, Chem. Mater. **15**, 1535 (2003).
[20]Z. Li, Y. Dong, B. Mi, Y. Tang, M. Häussler, H. Tong, P. Dong, J. W. Y. Lam, Y. Ren, H. H. Y. Sun, K. Wong, P. Gao, I. D. Williams, H. S. Kwok, and B. Z. Tang, J. Phys. Chem. B **109**, 10061 (2005).
[21]B.-K. An, S.-K. Kwon, S. D. Jung, and S. Y. Park, J. Am. Chem. Soc. **124**, 14410 (2002).
[22]B.-K. An, D.-S. Lee, J.-S. Lee, Y.-S. Park, H.-S. Song, and S. Y. Park, J. Am. Chem. Soc. **126**, 10232 (2004).
[23]Y. Liu, X. Tao, F. Wang, J. Shi, J. Sun, W. Yu, Y. Ren, D. Zou, and M. Jiang, J. Phys. Chem. C **111**, 6544 (2007).
[24]Y. Sonoda, S. Tsuzuki, M. Goto, N. Tohnai, and M. Yoshida, J. Phys. Chem. A **114**, 172 (2010).
[25]R. Hu, E. Lager, A. Aguilar-Aguilar, J. Liu, J. W. Y. Lam, H. H. Y. Sung, I. D. Williams, Y. Zhong, K. S. Wong, E. Pea-Cabrera, and B. Z. Tang, J. Phys. Chem. C **113**, 15845 (2009).
[26]G. Yu, S. W. Yin, Y. Liu, J. Chen, X. Xu, X. Sun, D. Ma, X. Zhan, Q. Peng, Z. Shuai, B. Tang, D. Zhu, W. Fang, and Y. Luo, J. Am. Chem. Soc. **127**, 6335 (2005).
[27]S. W. Yin, Q. Peng, Z. G. Shuai, W. H. Fang, Y. H. Wang, and Y. Luo, Phys. Rev. B **73**, 205409 (2006).
[28]Q. Peng, Y. P. Yi, Z. G. Shuai, and J. S. Shao, J. Am. Chem. Soc. **129**, 9333 (2007).
[29]Q. Peng, Y. Niu, C. M. Deng, and Z. G. Shuai, Chem. Phys. **370**, 215 (2010).
[30]Q. Peng, Y. P. Yi, Z. G. Shuai, and J. S. Shao, J. Chem. Phys. **126**, 114302 (2007).
[31]Y. Niu, Q. Peng, and Z. G. Shuai, Sci. China, Ser. B: Chem. **51**, 1153 (2008).
[32]Y. Niu, Q. Peng, C. M. Deng, X. Gao, and Z. G. Shuai, J. Phys. Chem. A **114**, 7817 (2010).
[33]A. Qin, J. W. Y. Lam, F. Mahtab, C. K. W. Jim, L. Tang, J. Sun, H. H. Y. Sung, I. D. Williams, and B. Z. Tang, Appl. Phys. Lett. **94**, 253308 (2009).
[34]B. Valeur, *Molecular Fluorescence: Principles and Application* (Wiley VCH, Weinheim, 2002).
[35]Q. Peng, Y. Niu, Z. Wang, Y. Jiang, Y. Li, Y. Liu, and Z. G. Shuai, J. Chem. Phys. **134**, 074510 (2011).
[36]S. H. Lin, C. H. Chang, K. K. Liang, R. Chang, Y. J. Shiu, J. M. Zhang, T.-S. Yang, M. Hayashi, and F. C. Hsu, Adv. Chem. Phys. **121**, 1 (2002).
[37]C.-P. Liu, J. J. Newby, C. W. Müller, H. D. Lee, and T. S. Zwier, J. Phys. Chem. A **112**, 9454 (2008).
[38]C. W. Müller, J. J. Newby, C.-P. Liu, C. P. Rodrigoa, and T. S. Zwier, Phys. Chem. Chem. Phys. **12**, 2331 (2010).
[39]S. H. Lin, J. Chem. Phys. **44**, 3759 (1966).
[40]W. Domcke, D. R. Yarkony, and H. Koppel, *Conical Intersections* (World Scientific, Singapore, 2004).
[41]M. Ben-Nun and T. J. Martinez, Chem. Phys. **259**, 237 (2000).
[42]A. D. Becke, J. Chem. Phys. **98**, 5648 (1993).
[43]C. Lee, W. Yang, and R. G. Parr, Phys. Rev. B **37**, 785 (1988).
[44]A. Schafer, H. Horn, and R. Ahlrichs, J. Chem. Phys. **97**, 2571 (1992).
[45]F. Weigend and R. Ahlrichs, Phys. Chem. Chem. Phys. **7**, 3297 (2005).
[46]A. Dreuw and M. Head-Gordon, Chem. Rev. **105**, 4009 (2005).
[47]L. Serrano-Andres and M. Merchan, J. Mol. Struct.: THEOCHEM **729**, 99 (2005).
[48]R. Ahlrichs, M. Baer, M. Haeser, H. Horn, and C. Koelmel, Chem. Phys. Lett. **162**, 165 (1989).
[49]O. Treutler and R. Ahlrichs, J. Chem. Phys. **102**, 346 (1995).
[50]F. Furche and R. Ahlrichs, J. Chem. Phys. **117**, 7433 (2002).
[51]M. J. Frisch, G. W. Trucks, H. B. Schlegel, *et al.*, GAUSSIAN 03, Rev. E.01, Gaussion, Inc., Wallingford, CT, 2004.
[52]See supplementary material at http://dx.doi.org/10.1063/1.3606579 for theoretical study of radiative and non-radiative decay processes in pyrazine derivatives.
[53]R. G. Mortimer, *Physical Chemistry*, 3rd ed. (Elsevier, Amsterdam, 2008).
[54]F. C. Spano and L. Silvestri, J. Chem. Phys. **132**, 094704 (2010).
[55]F. C. Spano, Acc. Chem. Res. **43**, 429 (2010).